



Available online at [www.sciencedirect.com](http://www.sciencedirect.com)



Journal of Volcanology and Geothermal Research 150 (2006) 119–131

Journal of volcanology  
and geothermal research

[www.elsevier.com/locate/jvolgeores](http://www.elsevier.com/locate/jvolgeores)

## On the absence of InSAR-detected volcano deformation spanning the 1995–1996 and 1999 eruptions of Shishaldin Volcano, Alaska

S.C. Moran<sup>a,\*</sup>, O. Kwoun<sup>b,1</sup>, T. Masterlark<sup>c,2</sup>, Z. Lu<sup>b,3</sup>

<sup>a</sup> U.S. Geological Survey, Cascades Volcano Observatory, 1300 SE Cardinal Ct., Bldg. 10, Vancouver, WA 98683, United States

<sup>b</sup> U.S. Geological Survey, EROS Data Center, SAIC, 47914 252nd Street, Sioux Falls, SD 57198, United States

<sup>c</sup> Department of Geological Sciences, University of Alabama, Tuscaloosa, AL 35487, United States

Received 1 June 2004; received in revised form 10 September 2004

Available online 8 September 2005

### Abstract

Shishaldin Volcano, a large, frequently active basaltic-andesite volcano located on Unimak Island in the Aleutian Arc of Alaska, had a minor eruption in 1995–1996 and a VEI 3 sub-Plinian basaltic eruption in 1999. We used 21 synthetic aperture radar images acquired by ERS-1, ERS-2, JERS-1, and RADARSAT-1 satellites to construct 12 coherent interferograms that span most of the 1993–2003 time interval. All interferograms lack coherence within ~5 km of the summit, primarily due to persistent snow and ice cover on the edifice. Remarkably, in the 5–15 km distance range where interferograms are coherent, the InSAR images show no intrusion- or withdrawal-related deformation at Shishaldin during this entire time period. However, several InSAR images do show deformation associated with a shallow  $M_L$  5.2 earthquake located ~14 km west of Shishaldin that occurred 6 weeks before the 1999 eruption. We use a theoretical model to predict deformation magnitudes due to a volumetric expansion source having a volume equivalent to the 1999 erupted volume, and find that deformation magnitudes for sources shallower than 10 km are within the expected detection capabilities for interferograms generated from C-band ERS 1/2 and RADARSAT-1 synthetic aperture radar images. We also find that InSAR images cannot resolve relatively shallow deformation sources (1–2 km below sea level) due to spatial gaps in the InSAR images caused by lost coherence. The lack of any deformation, particularly for the 1999 eruption, leads us to speculate that magma feeding eruptions at the summit moves rapidly (at least 80 m/day) from >10 km depth, and that the intrusion–eruption cycle at Shishaldin does not produce significant permanent deformation at the surface.

Published by Elsevier B.V.

**Keywords:** satellite interferometry; volcano deformation; deformation modeling; magma ascent rates; Shishaldin Volcano; Aleutian Islands

\* Corresponding author. Tel.: +1 360 993 8934; fax: +1 360 993 8980.

E-mail addresses: [smoran@usgs.gov](mailto:smoran@usgs.gov) (S.C. Moran), [okwoun@usgs.gov](mailto:okwoun@usgs.gov) (O. Kwoun), [masterlark@geo.ua.edu](mailto:masterlark@geo.ua.edu) (T. Masterlark), [lu@usgs.gov](mailto:lu@usgs.gov) (Z. Lu).

<sup>1</sup> Tel.: +1 605 594 6153.

<sup>2</sup> Tel.: +1 205 348 5095.

<sup>3</sup> Tel.: +1 605 594 6063.

## 1. Introduction

Satellite interferometric aperture radar (InSAR) has rapidly gained acceptance as an invaluable tool for detecting deformation at volcanic centers (e.g., Lu et al., 1997, 2002a,b; Wicks et al., 1998; Amelung et al., 2000; Zebker et al., 2000; Massonnet and Sigmundsson, 2000; Mann et al., 2002; Pritchard and Simons, 2002). One of the most important attributes of InSAR is the ability to provide a high-resolution map of a single deformation component over a time-span of months to years for volcanoes where little or no real-time deformation monitoring exists (e.g., volcanoes in the Galapagos, Ecuador (Amelung et al., 2000); Three Sisters, Oregon (Wicks et al., 2002); Peulik (Lu et al., 2002b), Westdahl (Lu et al., 2003a), Seguam (Masterlark and Lu, 2004), and Kiska (Lu et al., 2002a) volcanoes, Alaska; many volcanoes in the Central Andes (Pritchard and Simons, 2002)). To date, most studies have

focused on interpreting InSAR results that show some type of deformation, either associated with eruptive activity (e.g., the Galapagos; Okmok volcano, Alaska (Mann et al., 2002)) or intrusive activity (e.g., Peulik and Seguam volcanoes, Alaska; Three Sisters). In several cases the deformation pattern came as a surprise, since no other geophysical or geological signs of unrest were present (e.g., Three Sisters, Peulik, Kiska).

Here we present InSAR images bracketing two eruptions of Shishaldin, a basaltic-andesite volcano (Miller et al., 1998) located on Unimak Island, the easternmost Aleutian Island in Alaska (Fig. 1). The interferograms for Shishaldin are remarkable in that they show no evidence of deformation attributable to magma intrusion or withdrawal associated with either the 1995–1996 or 1999 eruptions. We use a theoretical model to demonstrate that significant net volume changes at 2–10 km depth equivalent to the volume erupted during the 1999 eruption should have pro-

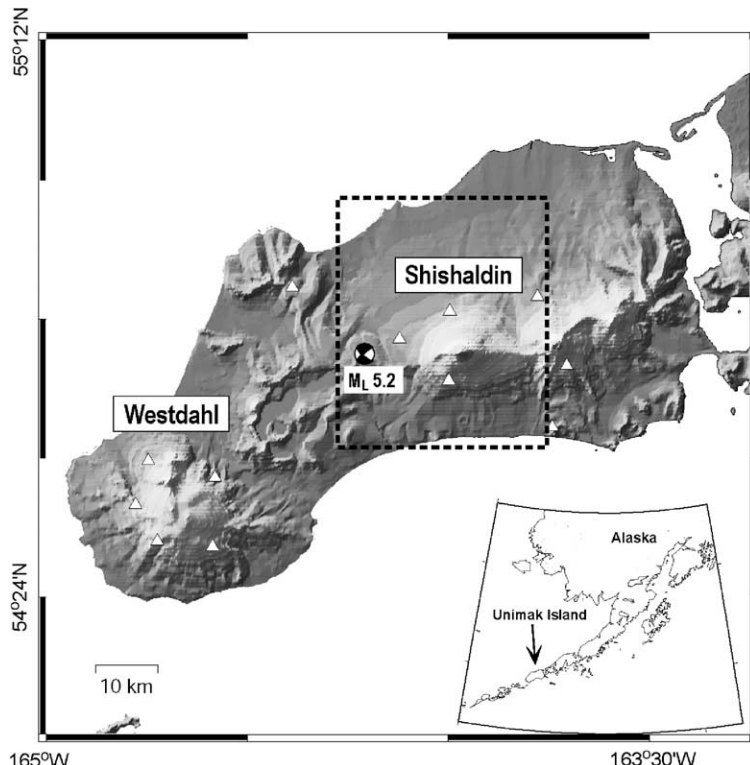


Fig. 1. Map showing location of Shishaldin and Westdahl volcanoes on Unimak Island, short-period seismic stations (triangles), and the location of the 4 March 1999  $M_L 5.2$  mainshock (circle). The dashed rectangle shows the area covered by Figs. 2–4.

duced deformation observable via InSAR. We suggest that the most likely explanation for lack of deformation is that any pre-eruptive deformation was canceled by post-eruptive deformation, implying that there was little net volumetric change in the upper part of the Shishaldin magmatic system as a result of the 1999 eruption.

## 2. Background

Shishaldin Volcano, with at least 18 eruptions reported in the 20th century (Miller et al., 1998; Nye et al., 2002), is one of the most frequently active volcanoes in the Aleutian volcanic arc. The steep-sided edifice, which rises to 2857 m above sea level, is the highest peak in the Aleutian Islands and has a small summit crater from which a steady plume has emitted for decades (Miller et al., 1998). Shishaldin typically produces mild-to-moderate Strombolian eruptions of basaltic to basaltic-andesite lava. However, on at least three occasions over the last 200 yr major explosive eruptions have occurred (Miller et al., 1998; Nye et al., 2002). Its two most recent eruptions were a mild Strombolian ash-and-steam eruption in 1995–1996 (Neal and McGimsey, 1997) and a Strombolian eruption in March–July 1999 that rapidly transformed into a sub-Plinian eruption on 19 April 1999 (Nye et al., 2002).

Shishaldin is monitored by a network of 12 short-period seismometers installed on Unimak Island (Fig. 1) by the Alaska Volcano Observatory (AVO) during the summers of 1997 and 1998 to monitor seismicity in real-time at Shishaldin, Westdahl, and several other volcanoes on Unimak Island (Jolly et al., 2001). Signals from these stations are telemetered in real-time to AVO. A campaign-style GPS network was established on Westdahl volcano in 1998 (Mann and Freymueller, 2003), but benchmarks have yet to be established around Shishaldin. Thus InSAR is the only source of deformation information available for Shishaldin.

AVO also monitors Shishaldin and all other Alaskan volcanoes via satellite remote sensing, using satellite imagery primarily from Geostationary Operations Environment Satellite (GOES) and Advanced Very High Resolution Radiometry (AVHRR) sensors. The nearest community with a view of Shishaldin is Cold

Bay, 90 km northeast of the volcano. Due to the remoteness of Shishaldin, satellite imagery was often the only means available for assessing the state of activity at Shishaldin and played a crucial role in enabling AVO to track the course of the 1995–1996 and 1999 eruptions (Nye et al., 2002).

## 3. The 1995–1996 and 1999 Shishaldin eruptions

The 1995–1996 eruption was apparently fairly small. It began with a short burst of steam and ash to an elevation of 10 km on 23 December 1995, depositing a light dusting of ash in Cold Bay (Nye et al., 2002). Two- to three-pixel (one pixel is ~1 km on a side) hot spots were observed in AVHRR images following this eruption through April and possibly May of 1996 (Neal and McGimsey, 1997). Activity in 1996 consisted largely of vigorous steaming, although AVO personnel observed a light dusting of fresh ash on the upper flanks and crater rim of Shishaldin on 16 May 1999 (Neal and McGimsey, 1997). The total volume of erupted material is unknown. No tephra deposits directly attributable to the 1995–1996 eruption have been found, but the net volume is thought to have been fairly small (P. Stelling, personal communication, 2004).

The 1999 eruption of Shishaldin probably began in early April, although a definitive start date is difficult to determine as no visual confirmation of the eruption was received until 17 April (Nye et al., 2002). The seismic unrest associated with the eruption arguably began in late June 1998 with a swarm of small-magnitude long-period (LP) events that continued through mid-August (Moran et al., 2002; Nye et al., 2002). Similar LP swarms also occurred in late September–late October of 1998 and late January–early February of 1999, although these had many fewer events than the first swarm (Moran et al., 2002). Well-constrained LP event locations mostly lie at shallow depths beneath the summit of Shishaldin, with several additional LP events occurring in June 1998 at depths >10 km (Moran et al., 2002; Power et al., 2004). Low-level seismic tremor was first identified in mid-January 1999, and was present on a relatively continuous basis through 19 April (Thompson et al., 2002). On 9 February a hot spot was identified in satellite imagery within the summit crater of Shishaldin (Nye et al.,

2002), indicating that magma was at or very near the surface by this time.

On 4 March 1999 a shallow ( $z=0$  km)  $M_L$  5.2 earthquake occurred ~14 km west of Shishaldin (Fig. 1), followed in subsequent weeks by over 900 located aftershocks. Moran et al. (2002) concluded from a Coulomb static stress change analysis that the mainshock could have been triggered by dike injection beneath Shishaldin. On 7 March observers in Cold Bay reported an unusual plume of turbulent air or gas jetting from the volcano to about 1.5 km above the vent before condensing to steam, suggesting that the hydrothermal system was energetic and high volume at this time (Nye et al., 2002). The first confirmation of eruptive activity at the summit was from an AVO observer on 17 April aboard an observation flight, who reported seeing Strombolian activity to 200 m above the summit (Nye et al., 2002). On 19 April tremor levels rapidly increased, culminating in a short-lived (~50 min) but explosive sub-Plinian eruption that sent ash to an elevation of 16,000 m (Nye et al., 2002; Stelling et al., 2002; Caplan-Auerbach and McNutt, 2003). A vigorous Strombolian summit eruption occurred on 23 April, and occasional ash plumes were observed through the end of May. The total erupted volume (dense rock equivalent) is estimated to have been  $1.4 \times 10^7 \text{ m}^3$  (Stelling et al., 2002), the largest eruption at Shishaldin since a multi-vent flank eruption in 1825.

## 4. InSAR observations and modeling

### 4.1. InSAR results

We obtained 21 synthetic aperture radar (SAR) images suitable for measuring surface deformation at Shishaldin (Table 1) from four different satellites, including three C-band satellites (ERS-1, ERS-2, RADARSAT-1, wavelength=5.67 cm) and one L-band (JERS-1, wavelength=23.5 cm). We used the two-pass InSAR approach (e.g., Massonnet and Feigl, 1998; Rosen et al., 2000) to produce 12 deformation interferograms with reasonably good coherence that collectively span most of the 1993–2003 time interval. Image acquisition times and associated imaging parameters are given in Table 1. The differences in incidence angle and orbit direction of these four satellites increase the chance of deformation signal detection, as they measure different components of deformation. The digital elevation model (DEM) used to produce the interferograms is the 1" (about 30-m posting) Shuttle Radar Topography Mission (SRTM) DEM. The 1" SRTM DEM has relative and absolute vertical accuracies of better than 10 and 16 m, respectively (Farr and Kobrick, 2000), resulting in no more than 1 cm of line-of-sight error in our interferograms.

The main edifice of Shishaldin (~5 km radius) is covered by snow and ice most of the year, and therefore does not maintain coherence for C-band ERS interferograms spanning more than a few days

Table 1  
SAR images used to generate the 12 interferograms shown in Figs. 2–4

Orbit 1	Date	Orbit 2	Date	$B_n$ (m)	Incidence Angle (°)	Track Angle (°)	Figure #
1-11425	19930921	1-22290	19951019	121	23.3	-166.5	2a
1-22290	19951019	2-18148	19981009	-145	23.3	-166.5	2b
2-12866	19971005	2-22385	19990801	74	23.3	-166.6	2c
2-18148	19981009	2-22516	19990716	-47	23.3	-166.5	2d
2-22886	19990905	2-27395	20000716	-44	24.0	-166.6	2e
2-23387	19991010	2-26894	20000611	23	23.3	-166.5	2f
3-08864	19930924	3-24680	19960815	-233	38.8	-169.6	3a
3-14795	19941025	3-35883	19980902	274	38.8	-169.6	3b
4-14844	19980908	4-18617	19990530	-199	44.3	-8.9	4a
4-14844	19980908	4-19646	19990810	-262	44.3	-8.9	4b
4-25820	20001015	4-41255	20030930	-31	44.3	-8.9	4c
4-35767	20020911	4-40912	20030906	261	44.2	-8.9	4d

Dates correspond to image acquisition times in yyyyymmdd format. Orbit numbers include the satellite ID (1 = ERS-1, 2 = ERS-2, 3 = JERS-1, and 4 = RADARSAT-1) and orbit on which the images were acquired.  $B_n$  is the component of the interferogram baseline that is perpendicular to the radar look angle at the image center. Track angle is the direction of orbit with respect to north.

(Fig. 2). The loss of coherence is also caused by the geometric distortion over slopes that are steeper than the SAR look angle (Table 1) due to the side-looking nature of SAR sensors. Volcanic deformation in the coherent areas for all interferograms is insignificant. However, deformation is observed in Fig. 2c and d (both spanning the 1999 eruption) in the epicentral area of the 4 March 1999  $M_L$  5.2 earthquake.

The summit area is also decorrelated in L-band JERS-1 interferograms (Fig. 3). We used JERS-1 data because L-band InSAR images usually have fewer incoherent areas than C-band images due to longer wavelengths (Rosen et al., 1996). As with the C-band ERS interferograms, in the areas with coherence (generally 5–15 km from the summit) we find no significant volcanic deformation before, during, or after the 1995–96 eruptions (Fig. 3a). We also see no deformation in Fig. 3b, which spans the first few months (June–early September 1998) of seismic unrest that preceded the 1999 eruption (Fig. 3b). Unfortunately, we were unable to generate JERS-1 InSAR images that spanned the entire 1999 eruption.

As with the ERS and JERS interferograms, the entire summit and most of the edifice is also decorrelated in C-band RADARSAT interferograms (Fig. 4) due to slope steepness and snow and ice cover. However, surface deformation related to the 4 March 1999 earthquake is apparent (outlined by black circles in Fig. 4a and b), similar to ERS interferograms that also span the mainshock (Fig. 2c and d). Other fringe patterns in Fig. 4b are most likely due to atmospheric delay anomalies. No volcano-wide deformation over Shishaldin can be seen in either of the 1998–99 interferograms (Fig. 4a and b). Post-eruption (2000–2003, Fig. 4c and d) interferograms also show no significant deformation around Shishaldin.

The lack of a deformation signal for the 1995–96 eruption is not too surprising given the small volume of erupted material. However, the presence of high-temperature pixels in satellite images for ~4 months during the 1995–1996 eruption and the report of fresh ash deposits in May 1996 indicate that at least some magma had been intruded and was resident fairly close to the surface for at least several months following the initial eruption. Much more surprising is the absence of magmatic deformation associated with the 1999 eruption. Figs. 2c,d and 4a,d show interferograms spanning 1- to 2-yr periods covering much of

the 1998 buildup and 1999 eruption. In all cases there is no pattern indicative of magma intrusion or withdrawal, despite the fact that a significant amount of magma moved through the system during this time. The only significant ground-surface deformation apparent in all 12 interferograms is in the epicentral area of the 4 March 1999  $M_L$  5.2 earthquake.

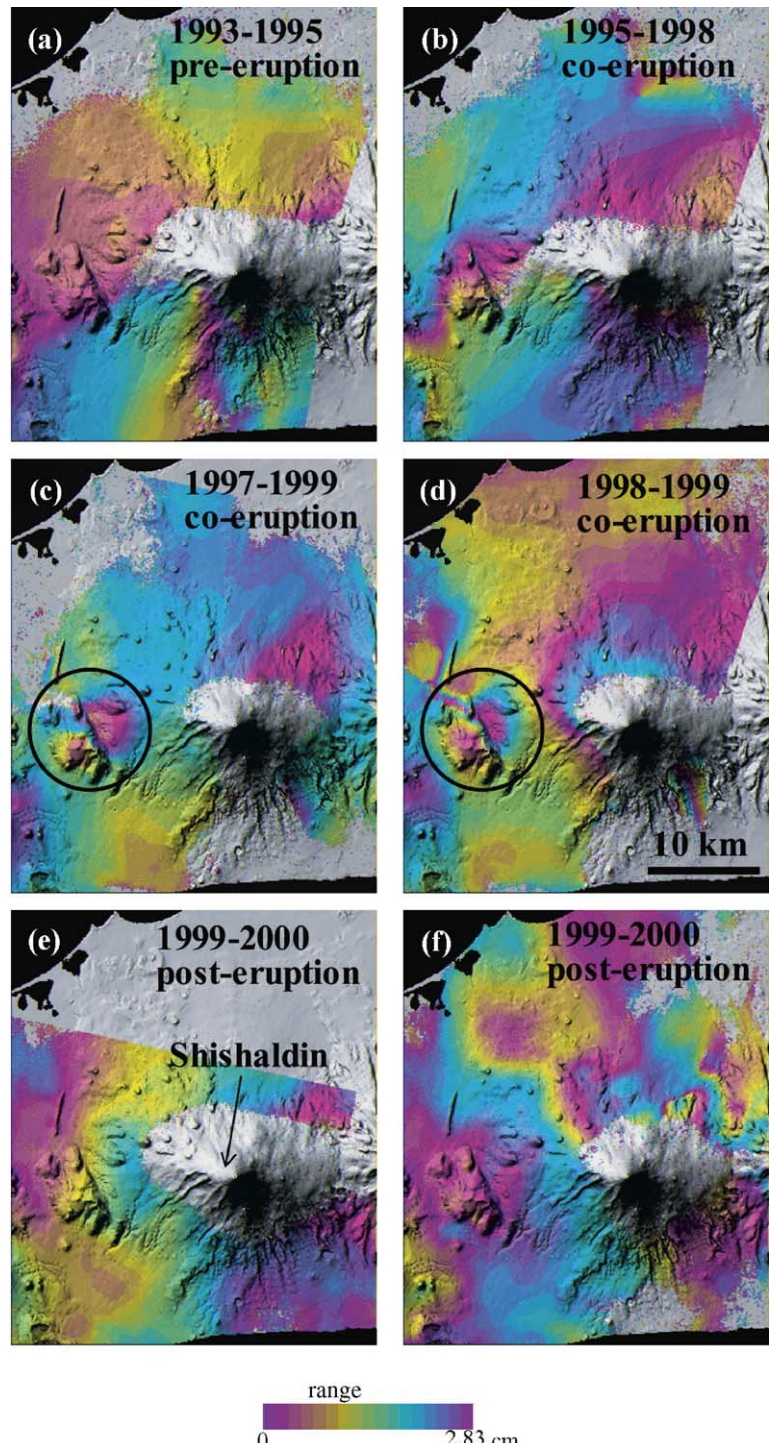
#### 4.2. Deformation modeling and the depth of source magma

The lack of evidence for deformation from InSAR images of the 1999 eruption in particular raises the question; under what conditions is it possible for a magma body of a given size to intrude into a magmatic system and not be detectable via InSAR? To address this question, we determined displacements at points around the volcano due to volumetric expansion of a source located beneath the summit at varying depths. The displacement of a point having location  $x$  at the surface of a homogeneous, isotropic, elastic half-space caused by a subsurface volumetric expansion-source located at  $\xi$  is

$$u_i(x_i, x_2, 0) = \Delta V \frac{(1-v)(1+v)}{2\pi(1-2v)} \times \frac{(x_i - \xi_i)}{\left[(x_1 - \xi_1)^2 + (x_2 - \xi_2)^2 + (-\xi_2)^2\right]^{3/2}} \quad (1)$$

where  $u$  is displacement,  $\Delta V$  is the expansion-source volume,  $v$  is Poisson's ratio, and  $i$  represents the three Cartesian coordinate indices (e.g., Masterlark and Lu, 2004). This expression is equivalent to Mogi (1958) solution for  $v=0.25$ .

We use this expression, corrected for topographic effects (Williams and Wadge, 1998), to calculate the predicted displacements for Shishaldin Volcano projected onto the line-of-sight (LOS) vector of the various satellites for coherent areas within 15 km from the summit, using  $\Delta V=1.4 \times 10^7 \text{ m}^3$  and  $v=0.3$  (Christensen, 1996). We assume a source located beneath the summit of Shishaldin, and only vary the source depth. The maximum relative differences between the LOS displacements for any two pixels (pixel size=40m) located within coherent zones are determined for source-depth increments of 100 m



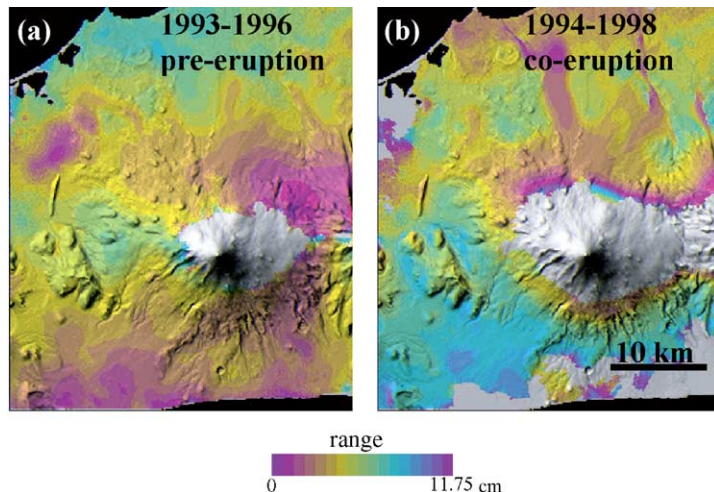


Fig. 3. Deformation interferograms of Shishaldin, constructed from L-band JERS-1 SAR images, for the periods (a) 24 September 1993 to 15 August 1996, and (b) 25 October 1994 to 2 September 1998 (both span the 1995–1996 eruption, and (b) spans the first three months of precursory seismicity prior to the 1999 eruption). Each fringe (a full color cycle) represents an 11.75 cm range change in the satellite look direction. Despite the relatively long wavelength of JERS-1, the summit area is decorrelated due to steep topography and snow and ice cover. A partial fringe around Shishaldin in (b) is probably due to atmospheric delay anomalies.

ranging from 0 to 30 km below sea level (BSL) (Fig. 5). These displacement predictions indicate that intrusion and/or withdrawal of magma could have occurred either at 1–2 km BSL or greater than 10 km BSL without resulting in displacements large enough to be detected via InSAR. Volume changes between 0 and 1 km BSL would be seen despite the lack of coherency within 5 km of the summit, as the deformation signal becomes large enough at shallow depths to extend out to regions with coherency.

On the other hand, interferograms spanning the 4 March 1999 mainshock (Figs. 2c,d and 4a,b) all show ground-surface deformation in the epicentral area of the  $M_L$  5.2 event. Masterlark et al. (2001) successfully modeled the fringe patterns with a fault plane oriented northeast–southwest, consistent with the location and focal mechanism determined by Moran et al. (2002). Both Masterlark et al. (2001) and Moran et al. (2002) demonstrated that the earthquake occurred in an area

where Coulomb stress was increased by several tenths of a bar, using theoretical models that assume an inflating dike beneath Shishaldin.

## 5. Discussion

### 5.1. Hypotheses for absence of InSAR deformation signal

The lack of evidence from InSAR for accumulated deformation over time periods bracketing the 1999 eruption is a surprise, although not unprecedented at erupting volcanoes. Zebker et al. (2000) found no evidence of deformation from InSAR studies of the 1995 eruption of Irruputuncu (Chile/Bolivia), the 30 April 1996 eruption of Popocatepetl (Mexico), the 1995 and 1996 eruptions of Pacaya (Guatemala), and the ongoing eruptions of Sakura-jima (Japan).

Fig. 2. Deformation interferograms of Shishaldin Volcano, constructed from C-band ERS-1 and ERS-2 SAR images, for the periods (a) 21 September 1993 to 19 October 1995, (b) 19 October 1995 to 9 October 1998 (spanning the 1995–1996 eruption), (c) 5 October 1997 to 1 August 1999 (spanning the 1999 eruption), (d) 9 October 1998 to 16 July 1999 (also spanning the 1999 eruption), (e) 5 September 1999 to 16 July 2000, and (f) 10 October 1999 to 11 June 2000. Any volcanic deformation over the coherent areas is insignificant. Deformation in the area enclosed by the circle in (c) and (d) is due to the 4 March 1999  $M_L$  5.2 earthquake that occurred ~6 weeks prior to the 1999 eruption. Interferograms are draped over DEM shaded-relief images. Areas without interferometric coherence are uncolored. Each fringe (a full color cycle) represents a 2.83 cm range change in the satellite look direction.

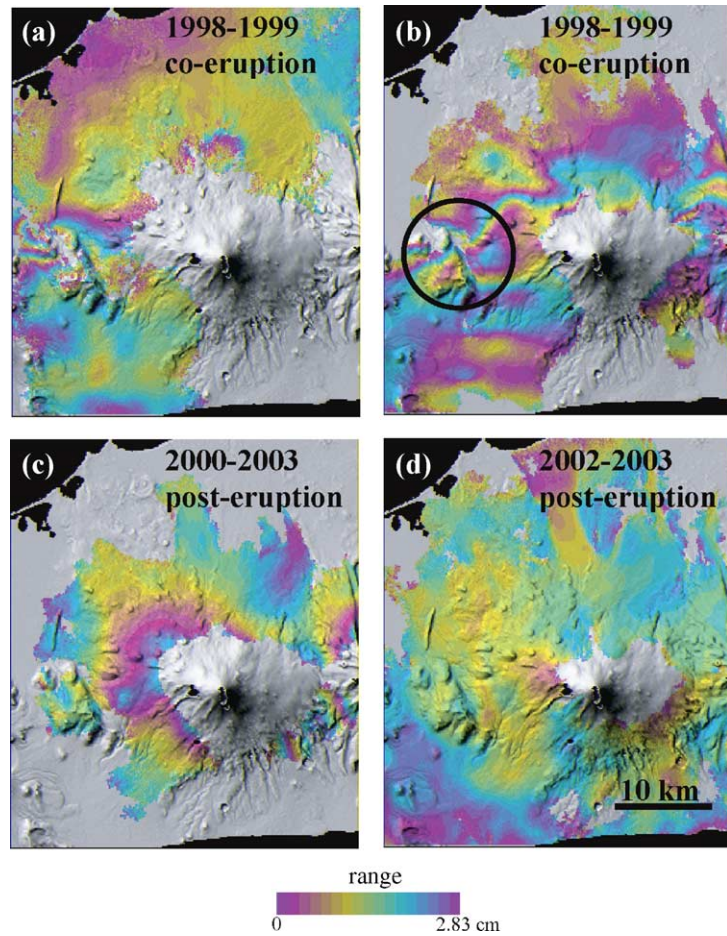


Fig. 4. Deformation interferogram of Shishaldin, constructed from C-band RADARSAT-1 SAR images, for the periods (a) 8 September 1998 to 30 May 30 1999 (spanning the 1999 eruption), (b) 8 September 1998 to 10 August 1999 (spanning the 1999 eruption), (c) 15 October 2000 to 30 September 2003, and (d) 11 September 2002 to 6 September 2003. Each fringe (a full color cycle) represents a 2.83 cm range change in the satellite look direction. The deformation over the area enclosed by the circle in (a) and (b) is due to the 4 March 1999  $M_L$  5.2 earthquake.

Pritchard and Simmons (2002) similarly found no deformation in InSAR images spanning three eruptions of Lascar (Chile) volcano, including one (April 1993) of similar size, duration, and type (Strombolian with several short Plinian phases) to the 1999 Shishaldin eruption (Smithsonian Institution, 1993). Finally, Lu et al. (2003b) found no deformation in interferograms spanning eruptions smaller than the 1999 Shishaldin eruption at Pavlof, Cleveland, and Korovin volcanoes in Alaska. Of these, the Lascar and Popocatepetl eruptions had volumes comparable to the 1999 Shishaldin eruption, with Lascar being the closest analog to Shishaldin in terms of eruption type and duration.

Several hypotheses can explain the lack of observed deformation at Shishaldin for the 1999 eruption: (1) pre-eruptive deformation occurred no earlier than 9 October 1998 and 30 May 1999 (the time of the latest pre-eruption SAR scene; Fig. 2c) and was balanced by post-eruptive deformation that occurred no later than 30 May 1999 (the time of the earliest post-eruption SAR scene; Fig. 4a), resulting in no observable net deformation; (2) The net volume changes occurred at  $>10$  km or 1–2 km BSL, depths at which our modeling results indicate magma intrusions and withdrawals can be hidden from InSAR; and (3) There was no significant ( $>2.83$  cm) pre- or post-eruptive deformation associated with either erup-

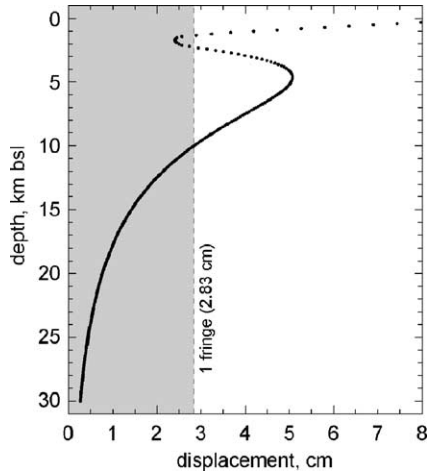


Fig. 5. Line-of-site (LOS) displacement versus source depth for a simple expansion-source model beneath the summit of Shishaldin. The model predicts the maximum relative LOS displacement, as a function of expansion-source depth, between coherent points within a 15 km radius of the summit. The expansion-source magnitude is  $1.4 \times 10^7 \text{ m}^3$  (Stelling et al., 2002) and predictions are corrected for topography (Williams and Wadge, 1998). The thin dashed line represents one fringe (2.83 cm) of relative LOS displacement. Relative displacements that lie within the gray region cannot be resolved unambiguously in C-band InSAR images (Figs. 2 and 4).

tion. We note that the first two hypotheses are not mutually exclusive.

We consider the third hypothesis the least likely for two reasons. First, if the  $M_L$  5.2 earthquake was in fact triggered by magma injection as suggested by Moran et al. (2002), then this suggests that there was some significant pre-eruptive deformation associated with 1999 eruption. Second, deformation has been observed via InSAR in association with similar-sized eruptions and intrusions at other volcanoes. For example, InSAR imagery clearly showed co-eruption deformation at radial distances of ~5 to 15 km associated with the 1991–1992 eruption of Westdahl volcano (Lu et al., 2003a), ~52 km west of Shishaldin (Fig. 1). An inverse analysis of the co-eruption InSAR image of Westdahl volcano suggests  $2 \times 10^7 \text{ m}^3$  of magma was withdrawn from a depth of 5.8 km BSL (Lu et al., 2003a). Another example comes from the 1995 eruption of Makushin volcano in Alaska, where interferograms spanning the hours-long phreatomagmatic eruption showed a two-year-long period of pre-eruptive inflation of a ~7-km-deep magma source with a volume change of  $\sim 2.2 \times 10^7 \text{ m}^3$  (Lu et al.,

2002a,b). Finally, Wicks et al. (2002) showed that fringes found in InSAR imagery from the Three Sisters volcanic field were best explained by a  $\sim 2.3 \times 10^7 \text{ m}^3$  magmatic intrusion at a depth of 6.5 km. The inferred magmatic volumes of all three cases are similar to that erupted from Shishaldin in 1999 ( $1.4 \times 10^7 \text{ m}^3$ ). Thus the lack of observed deformation for the 1999 eruption cannot be ascribed simply to a too-small volume of intruded or erupted magma.

While we acknowledge that the second hypothesis (all deformation occurred in InSAR blind zones) cannot be ruled out, this hypothesis alone is also not a likely explanation. The primary reason for this comes from the timeline and observations of the 1995–1996 and 1999 eruptions. We note that InSAR images show no net deformation occurring during any time from 1993 through 2003. It seems highly unlikely that magma withdrawal, which occurred twice during this time period, and magma intrusion, which likely occurred at least prior to the 1999 eruption, happened solely within the two blind zones at >10 km BSL and 1–2 km BSL. It is conceivable that the magma feeding these eruptions was only ‘old’ magma (i.e., intruded at some time prior to 1993) stored in the 1–2 km BSL blind zone. However, the combined volume for the two eruptions was larger than the  $1.4 \times 10^7 \text{ m}^3$  value used in our modeling. If the combined volume increases to  $1.7 \times 10^7 \text{ m}^3$  then the 1–2 km BSL blind zone in our theoretical model would disappear, resulting in at minimum one deformation fringe in all C-band interferograms (Figs. 2 and 4). Without this blind zone, the only regions where volume changes could have been hidden from InSAR were within the edifice and >10 km BSL, requiring that the eruptions tapped either deep or implausibly shallow magma bodies.

The most likely explanation is the first hypothesis, or a combination of the first two. We think it much more likely that both eruptions, particularly the 1999 eruption, were fed by new magma that moved rapidly from depth into a shallow reservoir from which it subsequently erupted. Evidence for this comes from the LP events that began in June 1998. A number of these LP events had depths greater than 10 km (Moran et al., 2002; Power et al., 2004). Deep LP (DLP) events also preceded the 1991 eruption of Mt. Pinatubo, and were linked to magma transport by White (1996). The DLP events at Shishaldin may similarly

indicate that transport of magma from mid-crustal depths began at this time.

If magma transport from depth began in June 1998, then enough magma had reached the near-surface by late January 1999 to produce hot spots in satellite imagery and activate the hydrothermal system, resulting in the relatively continuous low-amplitude tremor that began in early January and vigorous steam plumes that were first observed in early February (Nye et al., 2002; Dehn et al., 2002; Thompson et al., 2002). If the 4 March 1999 earthquake was caused by intrusion, then this could indicate that most or all of the erupted magma was in a near-surface storage reservoir by this time. The fact that this was the largest earthquake recorded in the area over the last 35 years suggests that this earthquake was preceded by the most significant intrusion event beneath Shishaldin over the last 35 yr, providing additional support for the idea that most of the magma erupted in 1999 moved upwards relatively rapidly from depth. Olivine phenocrysts found in the 1999 erupted products suggest that the magma resided at shallow depths (~3–5 km) for 10–1000 days (Stelling, personal communication, 2004). Geochemical evidence indicates that the erupted magma was largely degassed (Stelling et al., 2002), suggesting that it likely had been near the surface for some time, certainly longer than 10 days. Thus evidence from seismicity, geochemistry, satellite imagery, and visual observations are all consistent with the hypothesis that new magma rose relatively rapidly from depths greater than 10 km, and was resident in the near-surface for at least several months prior to eruption.

Even if no new magma entered the system from a deeper source, there had to be transport and short-term accumulation of magma between an upper-crustal reservoir and the summit prior to the 1999 eruption. Although some transport and accumulation undoubtedly occurred in one or all of the zones blind to InSAR, there also must have been transport in “observable zones” where volume changes would have created fringes in interferograms bracketing the 1999 eruptions. The lack of such fringes indicates that magma intrusion and transport through InSAR “observable zones” occurred relatively quickly (i.e., between pairs of SAR images spanning each eruption), and that intrusion was balanced by subsequent withdrawal of a roughly equivalent volume of magma,

leaving no net deformation field. In addition, it is also conceivable that net volume changes did occur in one or all of the blind zones.

In summary, the most likely explanation for the lack of observable deformation in InSAR imagery is that little net volume change occurred between 10 km BSL and sea level over the time-span of all interferograms spanning the 1999 eruption (Figs. 2c,d and 4a,b). One implication of this explanation is that the volume of magma that entered the part of the magmatic system to which InSAR is sensitive (0–10 km BSL) was roughly equivalent to the volume of magma withdrawn during the 1999 eruption. Another implication is that the majority of magma feeding the 1999 eruption moved from greater than 10 km depth to the near-surface, and ultimately the summit, in less than four months (the time interval between the first SAR image used in Fig. 2d and the first appearance of hot spots in satellite imagery). These considerations suggest magma transport rates of at least 80 m/day. Similarly rapid rates of magma migration have been observed elsewhere. For example, Rutherford and Hill (1988) found evidence for transport rates of ~300–1200 m/day from depths of ~7 km for dacitic magmas feeding the post-May 18, 1980, dome-building eruptions at Mount St. Helens. In addition, Linde et al. (1993) found evidence indicating that basaltic-andesite magma feeding the 1991 Hekla eruption rose from 4 km depth to the surface in 30 min. In comparison, a ~80 m/day transport rate for basaltic magma seems quite reasonable.

## 5.2. Comparison to Westdahl volcano

The magma intrusion–eruption cycle at Shishaldin appears to be significantly different from that at nearby Westdahl volcano, despite similarities in composition and tectonic settings. InSAR (Lu et al., 2000, 2003a) and campaign GPS studies (Mann and Frey-mueller, 2003) of Westdahl from 1991 to 2001 show that Westdahl has had a complex deformation history, divided into three periods: (1) lack of significant inflation in the months prior to its most recent eruption in 1991–1992; (2) deflation during the 1991–1992 fissure-style eruption; and (3) inflation from 1992 to 2001. These observations suggest a cycle of initially rapid post-eruption inflation rates that decline to the point of becoming negligible prior to the next

eruption (see Fig. 8 in Lu et al., 2003a). The high rates of inflation were apparently accompanied by very little seismicity (10 total earthquakes located by AVO between 1998 and 2001), although the Westdahl seismic network was not installed until 1998 (Jolly et al., 2001; Dixon et al., 2002). Thus magma recharge at Westdahl appears to be a long-term process, with gradual accumulation and long-term storage occurring at shallow levels in the crust.

In contrast, magma recharge at Shishaldin appears to be a relatively short-term process, with an apparent one-to-one relationship between volumes of intruded and erupted magmas. This balance results in no permanent deformation at the surface. In effect, the Shishaldin magmatic system appears to have zero net storage between the relatively fast episodes of intrusion and withdrawal. This is schematically shown in Fig. 6, which can be directly compared to Fig. 8 from Lu et al. (2003a). If our model is correct, then there is little significant increase or decrease in volume of any shallow magma reservoirs during or between eruptions. We note that the persistent steam plumes seen at Shishaldin for decades (Miller et al., 1998) are compelling evidence for the presence of at least some magma at shallow depths to provide heat for steam generation. Given the lack of long-term deformation, we infer that this reservoir is too shallow for volume changes to be detectable by InSAR, with eruptions occurring frequently enough (18 eruptions in the 20th century) to periodically replenish this reservoir. The lack of any volcano-related deformation between 1993 and 2003 argues that there is no significant replenishment of this shallow reservoir from a deeper source during non-eruptive time periods.

## 6. Conclusions

Twelve InSAR interferograms generated from 21 SAR images spanning 1993–2003 show no volcano-related deformation at Shishaldin Volcano, despite the occurrence of two eruptions during this time interval. Since the 1995–1996 eruption was minor, it is conceivable that any intrusions or withdrawals of magma were too small to generate significant deformation. However, the 1999 eruption produced  $1.4 \times 10^7 \text{ m}^3$  (dense rock equivalent) of eruptive products. Our models indicate that volume changes at 0–10 km BSL in the magmatic system equivalent to the volume erupted in 1999 should have been detectable by InSAR. The occurrence of a  $M_L 5.2$  earthquake six weeks before the sub-Plinian 19 April 1999 eruption, inferred by Moran et al. (2002) to have been triggered by dike intrusion beneath Shishaldin, is evidence that a significant volume of magma had intruded to shallow depths by this time. Deep LP earthquakes occurring in June of 1998 suggest that magma migration from >10 km depth began at this time, with magma transport rates of ~80 m/day occurring after 9 October 1998 (the date of the latest pre-eruption SAR image bracketing the 1999 eruption (Figs. 2c,d and 4a,b; Table 1)). We conclude that the 1998–1999 intrusion–eruption cycle resulted in minimal net volume changes in the shallow (0–10 km BSL) part of the magmatic system, that intrusions prior to eruption move rapidly (~80 m/day for the 1999 eruption) from depth prior to eruption, and that Shishaldin has effectively zero net storage at depths above 10 km between intrusion and eruption cycles.

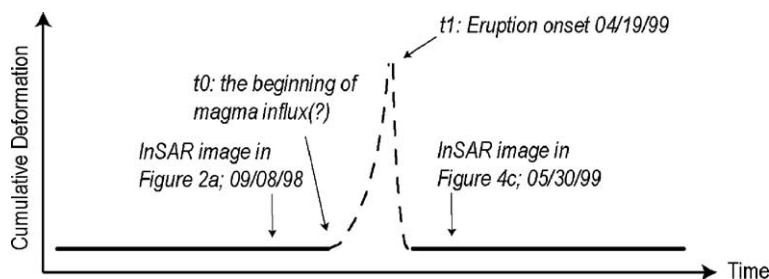


Fig. 6. Deformation model for magma intrusion–eruption cycles at Shishaldin. The model is based on the lack of observed deformation in the InSAR images bracketing the 19 April 1999 eruption (Figs. 2c,d and 4a,b). It implies rapid transport of magma from depth and effectively zero net storage or withdrawal of magma by each intrusion–eruption cycle.

## Acknowledgements

We are grateful for thorough and constructive reviews by Jackie Caplan-Auerbach, Paul Lundgren, Andrew Newman, Mike Poland, and an anonymous reviewer. In addition, Pete Stelling provided helpful responses to several key questions. We are also indebted to Guy Tytgat and others at the Alaska Volcano Observatory for their hard work installing and maintaining the Unimak Island seismic networks. ERS-1 and ERS-2, Radarsat-1, and JERS-1 SAR images are copyright © 1991–2003 European Space Agency (ESA), Canadian Space Agency (CSA), and Japan Aerospace Exploration Agency (JAXA), respectively, and were provided by the Alaska Satellite Facility (ASF) and JAXA. This research was supported by funding from the USGS Volcano Hazards Program, NASA (NRA-99-OES-10 RADARSAT-0025-0056), and in part by USGS contract O3CRCN0001. We thank ASF and JAXA for their excellent support in providing SAR data on a timely basis. Fig. 1 was generated using Generic Mapping Tools (GMT) software (Wessel and Smith, 1998).

## References

- Amelung, F., Jonsson, S., Zebker, H., Segall, P., 2000. Widespread uplift and ‘trapdoor’ faulting on Galapagos volcanoes observed with radar interferometry. *Nature* 407, 993–996.
- Caplan-Auerbach, J., McNutt, S.R., 2003. New insights into the 1999 eruption of Shishaldin volcano, Alaska, based on acoustic data. *Bull. Volcanol.* 65, 405–417.
- Christensen, N.I., 1996. Poisson’s ratio and crustal rheology. *J. Geophys. Res.* 101, 3139–3156.
- Dehn, J., Dean, K.G., Engle, K., Izbekov, P., 2002. Thermal precursors in satellite imagery of the 1999 eruption of Shishaldin Volcano. *Bull. Volcanol.* 64, 525–534.
- Dixon, J.P., Stihler, S.D., Power, J.A., Tytgat, G., Estes, S., Moran, S.C., Paskievitch, J., McNutt, S.R., 2002. Catalog of earthquake hypocenters at Alaskan Volcanoes: January 1, 2000 through December 31, 2001. U.S. Geol. Surv. Open-File Rep. 02-342 (56 pp.).
- Farr, T.G., Kobrick, M., 2000. Shuttle Radar Topography Mission produces a wealth of data. *Eos* 81, 583–585 (Fall Meeting Suppl.).
- Jolly, A.D., Stihler, S.D., Power, J.A., Lahr, J.C., Paskievitch, J., Tytgat, G., Estes, S., Lockhart, A.B., Moran, S.C., McNutt, S.R., Hammond, W.R., 2001. Catalog of earthquake hypocenters at Alaskan Volcanoes: January 1, 1994, through December 31, 1999. U.S. Geol. Surv. Open-File Rep. 01-189 (202 pp.).
- Linde, A.T., Agustsson, K., Sacks, I.S., Stefansson, R., 1993. Mechanism of the 1991 eruption of Hekla from continuous borehole strain monitoring. *Nature* 365, 737–740.
- Lu, Z., Fatland, R., Wyss, M., Li, S., Eichelberger, J., Dean, K., 1997. Deformation of volcanic vents detected by ERS-1 SAR interferometry, Katmai National Park, Alaska. *Geophys. Res. Lett.* 25, 1541–1544.
- Lu, Z., Wicks, C., Dzurisin, D., Thatcher, W., Freymueller, J.T., McNutt, S.R., Mann, D., 2000. Aseismic inflation of Westdahl volcano, Alaska, revealed by satellite radar interferometry. *Geophys. Res. Lett.* 27, 1567–1570.
- Lu, Z., Masterlark, T., Power, J.A., Dzurisin, D., Wicks, C., Thatcher, W., 2002a. Subsidence at Kiska volcano, western Aleutians, detected by satellite radar interferometry. *Geophys. Res. Lett.* 29, 1855, doi:10.1029/2002GL014948.
- Lu, Z., Wicks, C., Dzurisin, D., Power, J.A., Moran, S.C., Thatcher, W., 2002b. Magma inflation at a dormant stratovolcano: 1996–1998 activity at Mount Peulik volcano, Alaska, revealed by satellite radar interferometry. *J. Geophys. Res.* 107, doi:10.1029/2001JB000471.
- Lu, Z., Masterlark, T., Dzurisin, D., Rykhus, R., Wicks, C., 2003a. Magma supply dynamics at Westdahl volcano, Alaska, modeled from satellite radar interferometry. *J. Geophys. Res.* 108, 2354, doi:10.1029/2002JB002311.
- Lu, Z., Masterlark, T., Dzurisin, D., Power, J., Thatcher, W., Masterlark, T., 2003b. Interferometric synthetic aperture radar studies of Alaska volcanoes. *Earth Observation Magazine* 12 (3), 8–10, 12, 14, 16–18.
- Mann, D., Freymueller, J., Lu, Z., 2002. Deformation associated with the 1997 eruption of Okmok volcano, Alaska. *J. Geophys. Res.* 107, 2072, doi:10.1029/2001JB000163.
- Mann, D., Freymueller, J., 2003. Volcano and tectonic deformation on Unimak Island in the Aleutian Arc, Alaska. *J. Geophys. Res.* 108 (B2), 2108, doi:10.1029/2002JB001925.
- Massonnet, D., Feigl, K., 1998. Radar interferometry and its application to changes in the Earth’s surface. *Rev. Geophys.* 36, 441–500.
- Massonnet, D., Sigmundsson, F., 2000. Remote sensing of volcanic deformation by radar interferometry from various satellites. In: Mouginis-Mark, P.J., Crisp, J.A., Fink, J.H. (Eds.), *Remote Sensing of Active Volcanism*, Geophysical Monograph, vol. 116. American Geophysical Union, Washington, D.C., pp. 207–221.
- Masterlark, T., Lu, Z., 2004. Transient volcano deformation sources imaged with interferometric synthetic aperture radar: application to Seguam Island, Alaska. *J. Geophys. Res.* 109, B01401, doi:10.1029/2003JB002568.
- Masterlark, T., Lu, Z., Moran, S.C., Wicks, C., 2001. Inflation rate of Shishaldin volcano inferred from two-way stress coupling. *Eos* 82, F837 (Fall Meeting Suppl.).
- Miller, T.P., McGimsey, R.G., Richter, D.H., Riehle, J.R., Nye, C.J., Yount, M.E., Dumoulin, J.A., 1998. Catalog of the historically active volcanoes of Alaska. U.S. Geol. Surv. Open-File Rep. 98-582 (104 pp.).
- Mogi, K., 1958. Relations between the eruptions of various volcanoes and the deformations of the ground surface around them. *Bull. Earthquake Res. Inst. Univ. Tokyo* 36, 99–134.

- Moran, S.C., Stihler, S.D., Power, J.A., 2002. A tectonic earthquake sequence preceding the April–May 1999 eruption of Shishaldin Volcano, Alaska. *Bull. Volcanol.* 64, 520–524.
- Neal, C.A., McGimsey, R.G., 1997. 1996 volcanic activity in Alaska and Kamchatka: summary of events and response of the Alaska Volcano Observatory. U.S. Geol. Surv. Open-File Rep. 97-433 (41 pp.).
- Nye, C.J., Keith, T.E.C., Eichelberger, J.C., Miller, T.P., McNutt, S.R., Moran, S.C., Schneider, D.J., Dehn, J., Schaefer, J.R., 2002. The 1999 eruption of Shishaldin Volcano, Alaska: monitoring a distant eruption. *Bull. Volcanol.* 64, 507–519.
- Power, J.A., Stihler, S.D., White, R.A., Moran, S.C., 2004. Observations of deep long-period (DLP) seismic events beneath Aleutian Arc volcanoes; 1989–2002. *J. Volcanol. Geotherm. Res.* 138, 243–266.
- Pritchard, M., Simons, M., 2002. A satellite geodetic survey of large-scale deformation of volcanic centers in the central Andes. *Nature* 418, 167–171.
- Rosen, P., Hensley, S., Zebker, H., Webb, F., Fielding, E., 1996. Surface deformation and coherence measurements of Kilauea volcano, Hawaii, from SIR-C radar interferometry. *J. Geophys. Res.* 101, 23109–23125.
- Rosen, P.A., Hensley, S., Joughin, I.R., Li, F.K., Madsen, S.N., Rodriguez, E., Goldstein, R.M., 2000. Synthetic aperture radar interferometry. *Proc. IEEE* 88, 333–382.
- Rutherford, M.J., Hill, P.M., 1988. Magma ascent rates and magma mixing from amphibole breakdown: experiments and the 1980–1986 Mount St. Helens eruptions. *J. Geophys. Res.* 98, 19667–19685.
- Smithsonian Institution, 1993. Bulletin of the global volcanism network, vol. 18 (4). Smithsonian Institution, Washington, DC.
- Stelling, P., Beget, J., Nye, C.J., Gardner, J., Devine, J.D., George, R.M.M., 2002. Geology and petrology of ejecta from the 1999 eruption of Shishaldin Volcano, Alaska. *Bull. Volcanol.* 64, 548–561.
- Thompson, G., McNutt, S.R., Tytgat, G., 2002. Three distinct regimes of volcanic tremor associated with eruptions of Shishaldin Volcano, Alaska, April 1999. *Bull. Volcanol.* 64, 535–547.
- Wessel, P., Smith, W.H.F., 1998. New, improved version of the Generic Mapping Tools Released. *Eos* 79, 579.
- White, R.A., 1996. Precursory deep long-period earthquakes at Mount Pinatubo: spatio-temporal link to a basalt trigger. In: Newhall, C.G., Punongbayan, R.S. (Eds.), *Fire and Mud: Eruptions and Lahars of Mount Pinatubo, Philippines*. Univ. Washington Press, Seattle, pp. 307–328.
- Wicks, C., Thatcher, W., Dzurisin, D., 1998. Migration of fluids beneath Yellowstone Caldera inferred from satellite radar interferometry. *Science* 282, 458–462.
- Wicks, C., Dzurisin, D., Ingebritsen, S., Thatcher, W., Lu, Z., Iverson, J., 2002. Magmatic activity beneath the quiescent Three Sisters volcanic center, central Oregon Cascade Range, USA. *Geophys. Res. Lett.* 29, doi:10.1029/2001GL014205.
- Williams, C.A., Wadge, G., 1998. The effects of topography on magma chamber deformation models: application to Mt. Etna and radar interferometry. *Geophys. Res. Lett.* 25, 1549–1552.
- Zebker, H.A., Amelung, F., Jonsson, S., 2000. Remote sensing of volcano surface and internal processes using radar interferometry. In: Mouginis-Mark, P.J., Crisp, J.A., Fink, J.H. (Eds.), *Remote Sensing of Active Volcanism*, Geophysical Monograph, vol. 116. American Geophysical Union, Washington, D. C, pp. 179–205.